Induction of Redox Instability of Bovine Myoglobin by Adduction with 4-Hydroxy-2-nonenal†

A. L. Alderton,‡ C. Faustman,*,§ D. C. Liebler,|| and D. W. Hill⊥

Department of Animal Sciences, University of Kentucky, Lexington, Kentucky 40546-0215, Department of Animal Science, University of Connecticut, Storrs, Connecticut 06269-4040, Department of Pharmacology and Toxicology, University of Arizona, Tucson, Arizona, 85721, and Department of Pathobiology and Veterinary Sciences, University of Connecticut, Storrs, Connecticut 06269

Received November 13, 2002; Revised Manuscript Received February 7, 2003

ABSTRACT: The redox stability of myoglobin (Mb) is compromised by many factors, including lipid oxidation and its products. 4-Hydroxy-2-nonenal (HNE) is an α,β-unsaturated aldehyde derived from the oxidation of ω-6 polyunsaturated fatty acids and is highly reactive and cytotoxic. Our objective was to study potential binding of HNE to Mb and determine how it affects redox stability. OxyMb (0.15 mM) was incubated with HNE (1 mM) at 4, 25, and 37 °C at pH 7.4 or 5.6. Samples were analyzed for MetMb formation and by Western blot analyses, LC−MS, LC−MS−MS, circular dichroism (CD), and differential scanning calorimetry (DSC). MetMb formation increased with increasing temperature and was greater at pH 5.6 than at pH 7.4 ($P < 0.05$). At 37 °C, HNE accelerated oxidation at pH 7.4 but not at pH 5.6 ($P < 0.05$). At both 25 and 4 °C, HNE accelerated oxidation at pH 7.4 and 5.6 ($P < 0.05$). LC−MS revealed the covalent binding of HNE to Mb at both pH values via Michael addition, while Western blot analysis indicated that HNE was bound to histidine (HIS) residues. LC−MS−MS identified six histidine residues of Mb that were readily adducted by HNE, including the proximal (HIS 93) and distal (HIS 64) histidine associated with the heme group. Secondary structure differences between control Mb and Mb incubated with HNE were not detected by CD. However, DSC revealed a decreased T_m for Mb reacted with HNE at pH 7.4, indicating Mb tertiary structure was altered in a manner consistent with destabilization. These results suggest that HNE accelerates bovine skeletal muscle OxyMb oxidation in vitro by covalent modification at histidine residues.

Myoglobin (Mb), the major sarcoplasmic protein in skeletal muscle, is required for oxygen transport from hemoglobin to the terminal mitochondrial oxidase (*1*−*3*). Mb is a heme-containing protein comprised of 153 amino acids (MW = 17 800 Da) that can exist in three forms dictated by the redox state of the heme iron: ferrous deoxyMb and ferrous oxyMb or oxidized ferric MetMb (*4*). Physiologically, oxyMb and deoxyMb predominate; MetMb is converted to deoxyMb via the MetMb-reducing enzyme system (*5*). From a food product perspective, oxyMb is important because it is responsible for the bright cherry-red color observed in fresh meat. Once the MetMb-reducing system is depleted in post-mortem muscle, oxyMb oxidizes to MetMb and results in meat discoloration from red to brown. This undesirable oxidation process occurs naturally and from a retail perspective results in great economic loss to the meat industry.

The heme proteins, Mb and hemoglobin (Hb) readily autoxidize, a process that is affected by temperature (*6*), pH (*7*), metal ions (*8*), and a wide range of active oxygen species (*9*−*13*). Mb is a powerful catalyst of lipid oxidation known to oxidize a wide range of biological substrates including proteins in ischemic rat heart (*14*), human blood (*15*), estrogenic hormones (*16*), and arachidonic acid (*17*). During autoxidation, MetMb can be activated to a ferryl-heme (Fe^{4+}) protein that in the presence of cell membranes can initiate lipid peroxidation (*18*). Peroxides and free radicals can subsequently contribute to breakdown of the heme ring, thereby releasing iron to catalyze lipid oxidation (*19*, *20*).

Conversely, lipid oxidation and its products accelerate protein oxidation. Lipid metabolism leads to formation of reactive oxygen species and lipid radicals that decompose into secondary oxidation products capable of damaging macromolecules within the cellular environment (*21*−*23*). α,β-Unsaturated aldehydes are secondary products derived from ω-6 polyunsaturated fatty acid oxidation (*24*, *25*) that can react with cellular nucleophiles such as glutathione, DNA bases, and cysteine, lysine (LYS), and histidine residues of proteins (*26*). In particular, 4-hydroxy-2-nonenal (HNE) is a cytotoxic α,β-unsaturated aldehyde that accumulates in tissues exposed to oxidative conditions, including reperfused myocardium (*22*, *27*). HNE has been reported to inactivate glucose-6-phosphate dehydrogenase (*28*), decarboxylating

† This work was supported by USDA-NRI, USPHS Grants ES10056 and ES06694, and the Storrs Agricultural Experiment Station, University of Connecticut.

* To whom correspondence should be addressed. E-mail: cfaustma@canr.uconn.edu.

‡ University of Kentucky.

§ Department of Animal Science, University of Connecticut.

|| University of Arizona.

⊥ Department of Pathobiology and Veterinary Sciences, University of Connecticut.

10.1021/bi0271695 CCC: $25.00
Published on Web 03/26/2003

dehydrogenases (*29*), soybean lipoxygenase-1 (*30*), pyruvate dehydrogenase (*31*), cathepsin B (*32*), and insulin (*33*) through covalent modification of amino acids. In addition, HNE is implicated in pathophysiologic conditions such as atherosclerosis (*34*, *35*), Alzheimer's disease (*36*−*38*), Parkinson's disease (*39*), congestive heart failure (*40*), type 2 diabetes mellitus (*41*), sun-damaged skin (*42*), and renal failure (*43*, *44*).

The interaction of heme proteins and lipids has been an area of research interest in the medical and food sciences. In general, peroxides, peroxy radicals, and secondary oxidation products generated during lipid oxidation promote the accumulation of MetMb giving rise to the hypothesis that heme protein oxidation and lipid oxidation are interrelated (*18*, *45*−*47*). Clear support for the role of lipid oxidation in decreasing redox stability of ferrous OxyMb is provided by the observation that OxyMb stability is improved by the lipid soluble antioxidant α-tocopherol in liposomal and microsomal systems (*48*−*50*) and post-mortem bovine muscle (*51*, *52*). α-Tocopherol is known to prevent free radical damage by scavenging peroxy radicals and terminating free radical chain propagation (*53*− *55*). This would lead to a decreased rate of formation of reactive secondary oxidation products, such as HNE.

When different aldehydes were incubated with equine OxyMb, MetMb formation was greater in the presence of unsaturated aldehydes than with their saturated counterparts of equivalent carbon chain length (*47*). In addition, HNE accelerated equine MetMb formation in vitro; covalent modification of equine MetMb by HNE was confirmed using electrospray ionization mass spectrometry (ESI−MS) (*47*). Similarly, heme-free equine apoMb incubated with a 33-fold molar excess of HNE demonstrated from three to 10 HNE adducts to Mb via Michael addition to HIS residues (*56*).

The covalent binding of α,*β*-unsaturated aldehydes to OxyMb at key amino acid residues may subsequently lead to altered tertiary structure of the protein and increased susceptibility to oxidation. This would result in a loss of physiological activity and a red to brown discoloration in fresh meat. The effect of HNE on bovine Mb stability and the identification of the specific amino acids with which it reacts have not been investigated. Our objective was to study covalent binding of HNE to bovine Mb and determine its effects on redox stability.

EXPERIMENTAL PROCEDURES

Chemicals. Sephacryl S-200, ammonium sulfate, sodium hydrosulfite, sodium citrate, sodium phosphate, bicinchoninic acid (BCA) protein assay kit, ethanol, acetonitrile, trifluoroacetic acid (TFA), formic acid, and goat anti-mouse IgG alkaline phosphatase conjugate were obtained from Sigma Chem. Co. (St. Louis, MO). HNE was obtained from Cayman Chem. Co. (Ann Arbor, MI), and PD-10 columns were obtained from Pharmacia (Piscataway, NJ). Kits for SDS−PAGE and Western blots were obtained from Bio-Rad (Hercules, CA); sequence grade modified trypsin was obtained from Promega (Madison, WI). All chemicals were of reagent grade or greater purity.

Bovine Myoglobin Isolation and Purification. Bovine Mb was purified via ammonium sulfate precipitation and gel filtration chromatography according to Faustman and Phillips (*58*). Briefly, bovine longissimus dorsi muscle was homogenized in buffer (10 mM Tris-HCl, 1 mM EDTA, pH 8.0, 4 °C) and centrifuged at 5000*g* for 10 min. The supernatant was brought to 70% ammonium sulfate saturation and centrifuged at 18 000*g* for 20 min. The resulting supernatant was saturated with ammonium sulfate (100%) and centrifuged at 20 000*g* for 1 h. The precipitate was resuspended in homogenization buffer and dialyzed against 10 mM Tris-HCl, 1 mM EDTA, pH 8.0, 4 °C for 24 h. Mb was separated from hemoglobin using a Sephacryl S-200 gel filtration column (2.5 × 100 cm). The elution buffer contained 5 mM Tris-HCl, 1 mM EDTA, pH 8.0, 4 °C, and the flow rate was 60 mL/hr.

Oxymyoglobin Preparation. OxyMb was prepared by hydrosulfite-mediated reduction of purified bovine Mb, and residual hydrosulfite was removed by passing over a PD-10 column (*6*). The pH of Mb was adjusted to 5.6 and 7.4 with citrate (pH 5.6) or phosphate (pH.7.4) buffer dialysis, respectively.

Reaction of OxyMb with HNE and MetMb Formation. Bovine OxyMb (0.15 mM) was combined with HNE (1 mM) at 4, 25, and 37 °C at pH 5.6 and 7.4. Controls were aldehyde-free but contained an equivalent volume of ethanol (15 μL/mL) used to deliver HNE. Following incubation, unbound HNE was removed by passing over a PD-10 column. Samples were withdrawn from the incubation at various time periods for subsequent analysis. Reaction samples were scanned spectrophotometrically from 650 to 450 nm, and MetMb formation was calculated according to the method of Krzywicki (*59*).

SDS−PAGE and Western Blot Analyses. Sample preparation for SDS−PAGE followed the modified procedure of Fritz et al. (*60*). For Western blot analysis, Mb/HNE adducts were transferred from an unstained gel (15% acrylamide) to a 0.45 μm nitrocellulose membrane and treated as described by Fritz and Greaser (*61*). Monoclonal anti-4-HNE-histidine (1:50 dilution) (*62*) was used as a primary antibody while the secondary antibody was anti-mouse IgG alkaline phosphatase (AP) conjugate (1:10 000 dilution). Color was developed by incubation of membranes in substrate buffer (0.1 M Tris-HCl (pH 9.5), 0.1 M NaCl, 50 mM $MgCl_2$) containing AP color reagents nitroblue tetrazolium in aqueous dimethylformamide (DMF) and magnesium chloride and 5-bromo-4-chloro-3-indolyl phosphate in DMF (Bio-Rad Laboratories, Hercules, CA).

Mass Spectrometry. Liquid chromatography−mass spectrometry (LC−MS) and LC Tandem MS (LC−MS−MS) were used to analyze control Mb and Mb incubated with HNE prepared as described above. LC−MS samples were analyzed on a MicroMass Q-TOF II or Finnigan MAT TSQ 7000 mass spectrometer using positive electrospray ionization (ESI). Flow injection analysis was performed using acetonitrile/water (50:50, v/v) with 0.1% TFA at a flow rate of either 0.1 mL/min (MicroMass) or 0.2 mL/min (Finnigan). Collision-induced dissociation (CID) spectra were obtained using Ar as the collision gas at 30−50 eV collision energy. Prior to LC−MS−MS, samples were digested with sequencing grade modified porcine trypsin to yield peptides for spectral analysis (Promega, Madison, WI). The final protein concentration of trypsinized samples was 20 μg/mL as determined using a BCA protein assay kit. LC−MS with

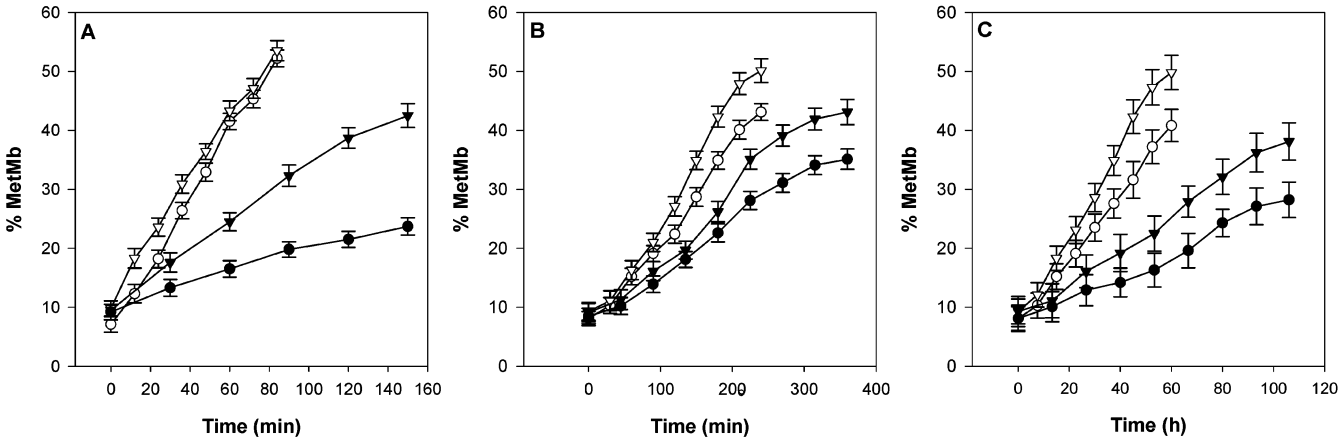

FIGURE 1: Bovine metmyoglobin (MetMb) formation during the reaction of oxymyoglobin (OxyMb; 0.15 mM) with 4-hydroxy-2-nonenal (HNE; 1 mM) at pH 7.4 or 5.6, 37 °C (A), 25 °C (B), or 4 °C (C). Standard error bars are indicated. Legend: −○−, pH 5.6, control; −▽−, pH 5.6, HNE; −●−, pH 7.4, control; −▼−, pH 7.4, HNE.

data dependent scanning and LC−MS−MS analyses were performed on a ThermoFinnigan LCQ ion trap mass spectrometer using positive ESI and flow injection in acetonitrile/water (50:50 v/v) with 0.1% TFA and 0.5% formic acid at a flow rate of 0.2 mL/min. A 10 μL injection volume was estimated to contain 0.2 μg of protein. Mb and Mb/HNE adducts were subsequently detected and confirmed using the protein database search software SEQUEST (*63*) and the SALSA algorithm (*64*, *65*) for ion series-based identification of MS−MS spectra corresponding to modified Mb sequences. In the study using ESI−MS to monitor the rate of Mb/HNE adduction, molecular ion spectra were generated using the maximum entropy algorithm, MaxEnt1 (Micromass Inc., Beverly, MA). Instruments were calibrated using commercial calibration standards.

Circular Dichroism. The CD spectra of Mb (0.01 mM) and Mb/HNE adducts were measured by scanning in a UV range of 190−300 nm using a Jasco J-720 spectropolarimeter (Japan Spectroscopic Co., Toxyo, Japan) and a Suprasil (Helma Cells, Jamaica, NJ) cuvette (0.2 cm light path) with a water jacket. Measurements of CD spectra were carried out at room temperature (25 °C) with a step of 1 nm and response of 0.5 ms.

Differential Scanning Calorimetry. High-sensitivity differential scanning calorimetry was performed using an MCS microcalorimeter (MicroCal Incorporated, Northampton, MA). The calorimetry cells were pressurized and heated from 30−95 °C at a rate of 1 °C/min. Heat capacity data were collected. Baseline stability was enhanced by performing several scans with buffer in each of the sample and reference cells until thermal equilibration was achieved. The experimental sample was then degassed, loaded into the sample cell, and scanned. The last buffer−buffer scan of the pre-experimental series was used as the instrument baseline. The temperature at peak heat capacity, T_m, was calculated to provide a measure of Mb stability. Mb concentrations for calorimetry experiments were adjusted to 1.25 mg/mL as determined using a BCA protein assay kit.

Statistical Analysis. MetMb formation data were analyzed by ANOVA using the general linear model (GLM) procedure of SAS (*66*). Significant differences ($P < 0.05$) among means were determined by the least significance difference test. Each reaction condition was performed in triplicate.

RESULTS AND DISCUSSION

The effect of HNE incubation on bovine MetMb formation at 37, 25, and 4 °C is presented in Figure 1. The reactions were completed at pH 7.4 (physiologic) or pH 5.6 (post-mortem bovine muscle). MetMb formation increased with increasing temperature and was greater at pH 5.6 than pH 7.4 ($P < 0.05$). At 37 °C (Figure 1A), a pro-oxidant effect of HNE relative to the control was observed at pH 7.4 but not at pH 5.6 ($P < 0.05$). Similar results were observed by Faustman et al. (*47*) during the incubation of HNE with equine OxyMb and by Lee et al. (*67*) with porcine OxyMb. It is well-documented that OxyMb autoxidation in vitro is enhanced at higher temperatures (*6*) and lower pH values (*7*). Bovine OxyMb autoxidation at pH 5.6 and 37 °C may have progressed rapidly enough to mask an observable redox destabilizing effect of HNE. When incubation temperature was lowered to either 25 or 4 °C (Figure 1B,C, respectively), Mb autoxidation was less rapid, and a clear redox destabilizing effect of HNE was observed at both pH 7.4 and pH 5.6.

Faustman et al. (*47*) utilized ESI−MS to demonstrate that HNE covalently attached to equine OxyMb and proposed that this could, in part, explain its effect on redox stability. To further investigate this hypothesis using bovine OxyMb, protein samples were incubated in the presence of HNE for 2 h at 37 °C, pH 7.4 and 5.6. LC−MS revealed the covalent binding of up to three molecules of HNE to Mb at pH 7.4 (Figure 2A), while at pH 5.6 up to two molecules of HNE were bound to Mb (Figure 2B). At both pH values, some Mb remained unadducted by HNE. These results also indicate that HNE adducts were formed via Michael addition as the adduct peaks corresponded to the mass of myoglobin plus 156 Da, the molecular mass of HNE. Schiff base formation between HNE and an appropriate nucleophile would have resulted in a molecular mass addition of 138 Da (i.e., addition followed by loss of water, 18 Da), and this was not observed. It is likely that adduct formation was greater at pH 7.4 because at pH 5.6 a greater proportion of ionizable groups would be charged and therefore less reactive.

The temporal rate of HNE adduction to bovine Mb was monitored by ESI−MS analysis of Mb samples incubated with HNE at 37 °C and pH 7.4 (Figure 3A) or pH 5.6 (Figure 3B). At pH 7.4, initial time points revealed the presence of native Mb only with no evidence of Mb/HNE formation.

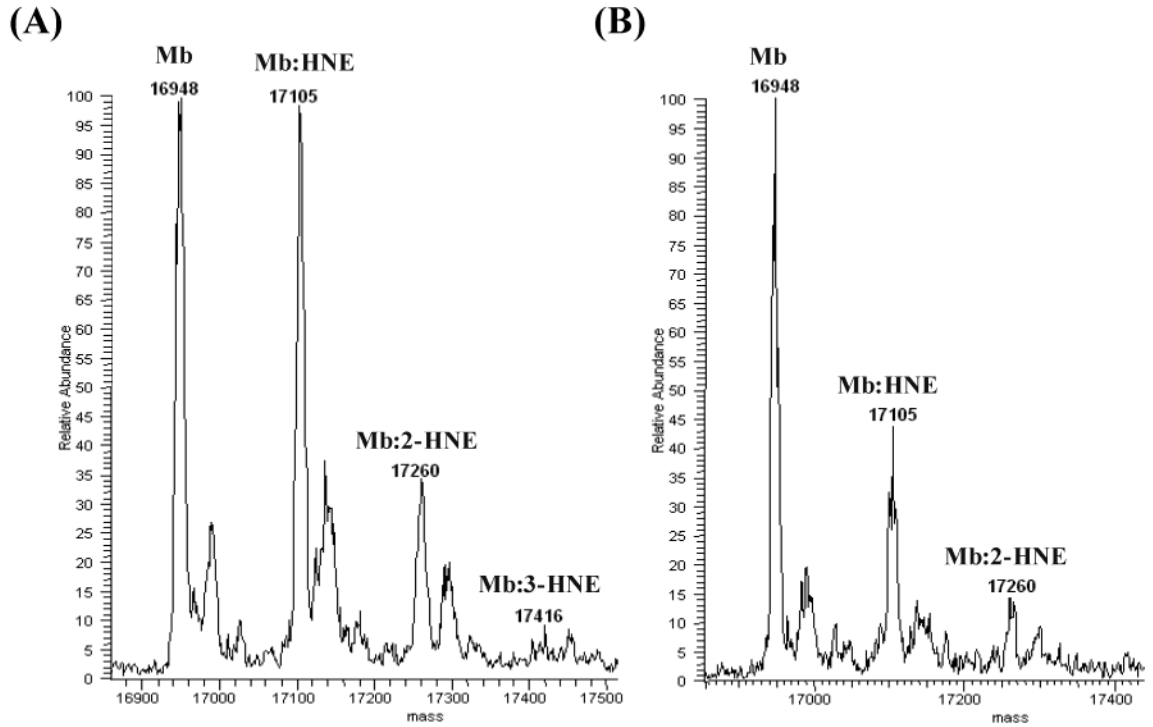

FIGURE 2: Deconvoluted LC−MS spectra of bovine myoglobin (Mb; 0.15 mM) following reaction with 4-hydroxy-2-nonenal (HNE; 1 mM) at pH 7.4 (A) or pH 5.6 (B) for 120 min at 37 °C.

However, following 15 min incubation with HNE, mono-adducts of Mb/HNE were detected (Figure 3A). Di-adducts (Mb/2-HNE) were observed after 90 min of incubation, and tri-adducts (Mb/3-HNE) began to form after 180 min of incubation. Following prolonged HNE incubation, a quad-adduct (Mb/4-HNE) was observed. A similar pattern of adduction was detected at pH 5.6 (Figure 3B); however, Mb/HNE formation did not occur as quickly as was observed at pH 7.4. HIS residues would be expected to be partially charged at pH 5.6 relative to pH 7.4, and their ability to serve as nucleophiles for reaction with HNE would be impaired (*68*).

It is not possible to identify the specific location of HNE adducts by ESI−MS of intact proteins. For a given adduct ratio (i.e., mono-, di-, tri-), HNE adduct mass ion peaks may represent several different Mb/HNE adducts, each with HNE bound to a potentially different amino acid. The nucleophilic amino acids cysteine, lysine, and histidine, as well as the protein N-terminal amine would be expected to be most reactive (*33*, *56*). Bovine Mb lacks cysteine residues (*69*), and the primary nucleophile candidates thus would be histidine and lysine and the N-terminal amine. Using a monoclonal antibody specific for histidine/HNE adducts (*62*), Western blot analysis confirmed the binding of HNE to bovine Mb histidine residues at 25 °C, pH 5.6 (Figure 4) and pH 7.4 (results not shown). The intensity of Mb/HNE adduct bands increased with incubation indicating increased adduct formation with time.

To determine the specific amino acid site(s) of HNE adduction, bovine Mb incubated with and without (control) HNE was digested with trypsin to obtain peptides of appropriate size for LC−MS−MS. The MS−MS data were analyzed with Sequest (*63*) and SALSA as described previously (*64*, *65*, *70*) to identify spectra corresponding to

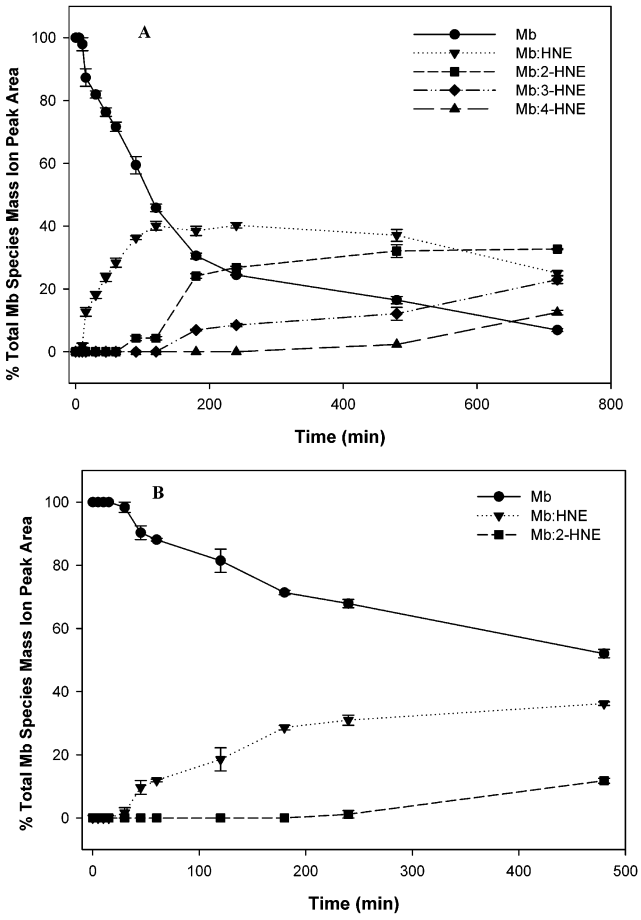

FIGURE 3: Formation of bovine myoglobin/4-hydroxy-2-nonenal (Mb/HNE) adducts and disappearance of native Mb was quantified by ESI−MS following incubation at 37 °C, pH 7.4 (A) or pH 5.6 (B).

Table 1: MS−MS Spectral Features of Unadducted and HNE-Adducted Myoglobin Peptides

peptide[a]	modification[b]	precursor (*m*/*z*)	b/y-ions detected[c]
17−31	unadducted	797.2	300.2 (b_3), 415.1 (b_4), 585.3 (b_6), 779.4 (b_8), 836.6 (b_9), 964.7 (b_{10}), 1192.6 (b_{12}), 1418.8 (b_{12}); 288.2 (y_2), 401.3 (y_3), 500.3 (y_4), 629.5 (y_5), 757.6 (y_6), 814.4 (y_7), 951.6 (y_8), 1008.6 (y_9), 1079.6 (y_{10}), 1178.8 (y_{11}), 1293.8 (y_{12})
17−31	+HNE	875.2	414.9 (b_4), 585.2 (b_6), **935.3 (b_8), 1120.5 (b_{10}), 1250.6 (b_{11}), 1461.7 (b_{13}), 1574.6 (b_{14})**; 287.9 (y_2), 401.3 (y_3), 500.3 (y_4), 629.4 (y_5), 757.6 (y_6), 814.5 (y_7), **1107.7 (y_8), 1164.6 (y_9), 1235.7 (y_{10}), 1334.7 (y_{11}), 1449.8 (y_{12})**
64−77	unadducted	697.5	309.2 (b_3), 410.2 (b_4), 509.2 (b_5), 622.4 (b_6), 794.5 (b_8), 907.5 (b_9), 964.5 (b_{10}), 1021.7 (b_{11}), 1247.7 (b_{13}); 373.4 (y_3), 430.3 (y_4), 487.5 (y_5), 600.4 (y_6), 772.5 (y_8), 984.6 (y_{10}), 1085.7 (y_{11}), 1199.8 (y_{12})
64−77	+HNE	775.6	294.1 (b_1), 351.2 (b_2), 466.8 (b_3), 566.1 (b_4), 665.2 (b_5), 950.4 (b_8), 1063.5 (b_9), 1120.5 (b_{10}), 1178.4 (b_{11}), 1291.7 (b_{12}), 1403.6 (b_{13}); 430.5 (y_4), 487.2 (y_5), 772.3 (y_8), 985.5 (y_{10}), 1199.5 (y_{12}), 1256.6 (y_{13})
88−96	unadducted	503.9	251.1 (b_2), 322.2 (b_3), 451.5 (b_4), 538.2 (b_5), 675.3 (b_6), 746.5 (b_7), 988.5 (b_9); 261.2 (y_2), 332.4 (y_3), 469.3 (y_4), 556.3 (y_5), 685.4 (y_6), 756.3 (y_7), 869.5 (y_8)
88−96	+HNE	581.7	251.1 (b_2), 322.2 (b_3), 451.6 (b_4), **831.4 (b_6), 902.4 (b_7)**; 261.1 (y_2), 332.2 (y_3), **625.4 (y_4), 712.4 (y_5), 912.4 (y_7), 1025.4 (y_8)**
103−118	unadducted	935.3	406.2 (b_3), 553.3 (b_4), 666.5 (b_5), 868.4 (b_7), 939.5 (b_8), 1052.5 (b_9), 1302.7 (b_{11}), 1401.8 (b_{12}), 1514.9 (b_{13}); 355.4 (y_3), 468.3 (y_4), 567.4 (y_5), 704.5 (y_6), 817.5 (y_7), 930.7 (y_8), 1001.7 (y_9), 1203.7 (y_{11}), 1463.9 (y_{13}), 1592.9 (y_{14})
103−118	+HNE	1013.2	406.0 (b_3), 939.9 (b_8), 1052.2 (b_9), 1303.1 (b_{11}), 1401.1 (b_{12}), 1514.8 (b_{13}); 511.2 (y_3), 625.4 (y_4), 723.4 (y_5), 860.5 (y_6), 1087.6 (y_8), 1157.6 (y_9), 1359.6 (y_{11}), 1749.6 (y_{14})
119−133	unadducted	767.1	322.3 (b_3), 437.2 (b_4), 584.3 (b_5), 641.4 (b_6), 712.3 (b_7), 898.4 (b_9), 1097.7 (b_{11}), 1299.5 (b_{13}); 436.3 (y_4), 507.3 (y_5), 706.4 (y_7), 821.4 (y_8), 949.5 (y_{10}), 1211.6 (y_{12}), 1298.7 (y_{13})
119−133	+HNE	845.22	293.9 (b_1), 391.2 (b_2), 740.2 (b_5), 797.2 (b_6), 1054.5 (b_9), 1182.5 (b_{10}), 1455.5 (b_{13}); 507.3 (y_5), 706.2 (y_7), 821.0 (y_8), 949.8 (y_{10}), 1096.5 (y_{11}), 1211.5 (y_{12}), 1298.5 (y_{13}), 1395.5 (y_{14})
148−153	unadducted	707.5	270.2 (b_3), 417.3 (b_4), 554.4 (b_5), 611.3 (b_6); 360.2 (y_3), 417.2 (y_4), 530.3 (y_5)
148−153	+HNE	785.3	270.2 (b_3), 417.3 (b_4), **710.2 (b_5), 767.2 (b_6)**; 369.2 (y_2), 516.2 (y_3), 573.2 (y_4), 686.2 (y_5)

[a] Amino acid positions in the bovine myoglobin target peptide. [b] The modification is HNE, 4-hydroxy-2-nonenal (M + 156). [c] Observed signals assigned as b- or y-ions are listed. Ions containing an adduct moiety are mass-shifted with respect to the corresponding ions in unmodified peptides and are listed in boldface.

FIGURE 4: Western blot analysis of bovine oxymyoglobin/4-hydroxy-2-nonenal (Mb/HNE) adducts formed following incubation at pH 5.6, 25 °C. Lanes 1, 3, 5, and 7 are aldehyde-free samples while lanes 2, 4, 6, and 8 are Mb/HNE samples incubated for 1, 2, 3, or 4 h, respectively. The arrow indicates Mb/HNE adducts as visualized with anti-HNE-histidine monoclonal antibody and anti-mouse IgG alkaline phosphatase conjugate (*62*).

unadducted and adducted Mb peptides. This approach identified six nucleophilic histidine residues confirmed to be adducted with HNE. HIS 24, 64, 93, 116, 119, and 152 each had a mass addition equivalent to that of HNE (i.e., 156 Da). Table 1 summarizes the b- and y-series ions for the six peptides identified to have HNE adductions. Sodium borohydride reduction of Mb prior to trypsin treatment was performed in an attempt to stabilize potential lysine/HNE Schiff base adducts for subsequent detection, but no lysine modifications were identified in these samples. Bolgar and Gaskell (*56*) studied HNE adduction of equine apoMb and determined that it occurred exclusively at histidine residues. In a related study (*34*), they incubated equine apoMb with a 33-fold molar excess of HNE for 2 h at 37 °C. A range of 3−10 HNE adducts per apoMb were identified, and LC−MS−MS revealed that Michael addition of HNE occurred at histidine residues only.

LC−MS−MS spectra of multiple early time point incubations (i.e., <2 h at 37 °C) indicated that HIS 64 and 93 were more readily adducted by HNE. This observation was based on the appearance of adducts at HIS 64 and 93 in bovine Mb samples incubated with HNE for ≤30 min. When attempts were made to identify HNE adducts at other amino acid residues, adducts were not found, indicating that HNE preferentially reacted with HIS 64 and 93. This result is interesting as HIS 93, the proximal histidine, is bound to the heme moiety of Mb. In addition, HIS 64, the distal histidine, coordinates with oxygen or other molecules associated with the sixth ligand during the interconversion of Mb redox forms (i.e., OxyMb and MetMb). Because HIS 93 and 64 lie in close proximity to the heme group, their modification by HNE could be expected to alter the protein structure around the heme cleft and subsequently impact redox stability. Figure 5 depicts the three-dimensional structure of bovine Mb adapted from the Molecular Modeling Database (MMDB) of the National Center for Biotechnology Information (www.ncbi.nlm.nih.gov). The six histidine/HNE adducts identified through MS−MS are mapped to their respective locations on the protein.

We attempted to characterize potential structural changes in Mb caused by HNE. Circular dichroism was used to assess potential changes in Mb secondary structure; however, no significant differences were observed between control protein and Mb incubated with HNE at pH 7.4 or 5.6 (results not shown).

Differential scanning calorimetry revealed changes in melting behavior of control and Mb reacted with HNE. At pH 7.4, control Mb exhibited a T_m of 79.8 °C with aggregation occurring at 84.5 °C (Figure 6A). No change in T_m occurred following 1 h incubation with HNE. However, after 2 h incubation, T_m decreased to 78.0 °C with protein aggregation beginning at approximately 68 °C. Following 8 h incubation with HNE, the protein aggregated very quickly with initiation of the heating cycle and indicated that HNE adduction compromised bovine Mb stability. No difference in T_m was observed between control and HNE-treated samples at pH 5.6 (Figure 6B). Rather, the protein appeared

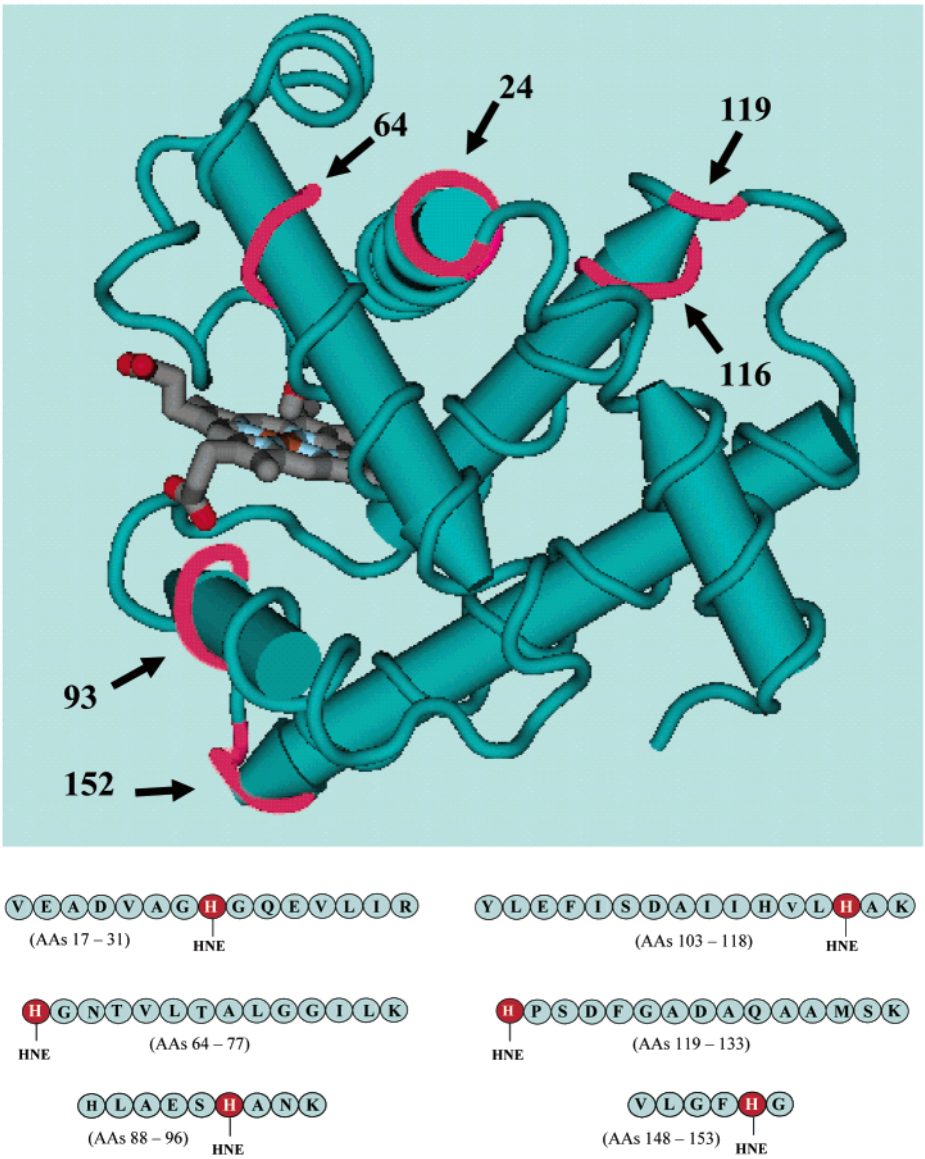

FIGURE 5: Three-dimensional structure of bovine myoglobin (Mb) and six common 4-hydroxy-2-nonenal (HNE) adducts. HNE adducts, all of which occur at histidine residues, are labeled. The three-dimensional structure was adapted from the Molecular Modeling Database (MMDB) of the National Center for Biotechnology Information (www.ncbi.nlm.nih.gov).

to be destabilized initially (i.e., prior to the melting process) as aggregation occurred early during the heating cycle.

This study reinforces the potential interaction between bovine Mb and lipid oxidation that may be partially explained by α,β-unsaturated aldehyde adduction, for which HNE serves as a model. We have demonstrated that HNE accelerates bovine OxyMb oxidation, and the covalent binding of HNE to histidine residues appears to facilitate this. Circular dichroism did not reveal secondary structural changes resulting from HNE incubation. However, the decrease in T_m detected by differential scanning calorimetry indicated that Mb tertiary structure was altered in a manner consistent with destabilization. On the basis of our analyses, perturbations in Mb structure resulting from HNE adduction appeared minor but significantly accelerated Mb oxidation.

HNE, a secondary product of lipid oxidation, accelerated bovine skeletal muscle OxyMb oxidation in vitro and appears to do so, in part, via covalent modification of multiple histidine residues (i.e., HIS 24, 64, 93, 116, 119, and 152). Although the adduction of HNE to Mb did not appear to alter OxyMb secondary structure as assessed by circular dichroism, heme-protein destabilization at pH 7.4 was detected using differential scanning calorimetry. This may offer a partial explanation for the previously noted acceleration of heme protein oxidation in the presence of aldehydes known to be produced from oxidizing lipids.

ACKNOWLEDGMENT

We thank Dr. George Tsaprallis and Jeanne Burr, Pharmacology and Toxicology, University of Arizona, Tucson and Al Kind, Pathobiology and Veterinary Sciences, University of Connecticut, for their expertise in mass spectrometry analysis. In addition, we thank Dr. Georg Waeg, Biochemistry and Microbiology, University of Graz, Austria, for his generous donation of anti-4-hydroxynonenal-histidine antibody and Dr. Larry Silbart, Animal Science, University of Connecticut, for guidance during Western blot analyses. Finally, we appreciate the guidance of Drs. C. V. Kumar and D. Kalonia during circular dichroism and differential scanning calorimetry analyses, respectively.

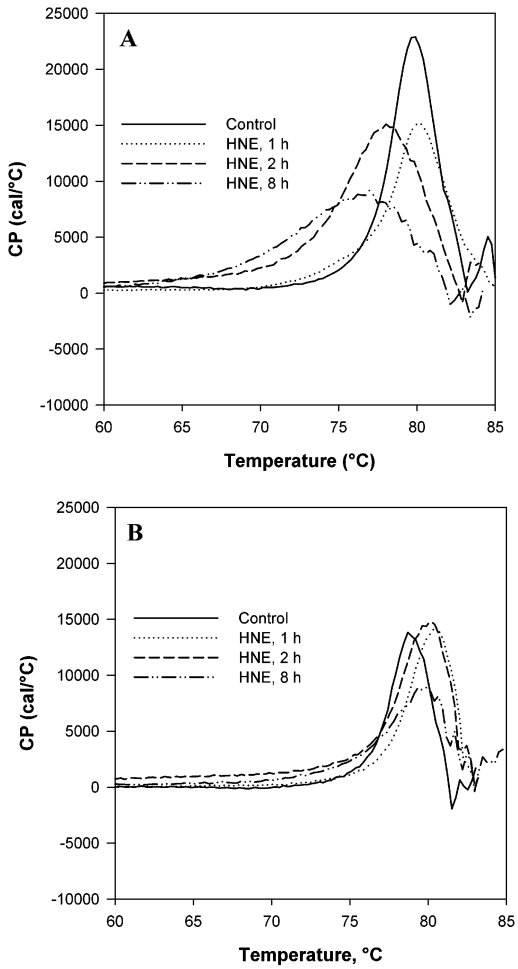

FIGURE 6: Differential scanning calorimetry of bovine oxymyoglobin/4-hydroxy-2-nonenal (Mb/HNE) adducts following incubation at 37 °C, pH 7.4 (A) or pH 5.6 (B).

REFERENCES

1. Antonini, E., and Brunori, M. (1971) *Hemoglobin and Myoglobin in Their Reactions with Ligands*, Elsevier, New York.
2. Esquerra, R. M., Goldbeck, R. A., Kim-Shapiro, D. B., and Kliger, D. S. (1998) Spectroscopic evidence for nanosecond protein relaxation after photodissociation of myoglobin-CO, *Biochemistry 37*, 17527−17536.
3. Wittenberg, B. A., and Wittenberg, J. B. (1989) Transport of oxygen in muscle, *Annu. Rev. Physiol. 57*, 857−878.
4. Antonini, E. (1965) Interrelationship between structure and function in hemoglobin and myoglobin, *Physiol. Rev. 45*, 123−170.
5. Hagler, L., Coppes, R. I., and Herman, R. H. (1979) Metmyoglobin reductase. Identification and purification of a reduced nicotinamide adenine dinucleotide-dependent enzyme from bovine heart which reduces metmyoglobin, *J. Biol. Chem. 254*, 6505−6511.
6. Brown, W. D., and Mebine, L. D. (1969) Autoxidation of oxymyoglobins, *J. Biol. Chem. 244*, 6696−6701.
7. Goto, T., and Shikama, K. (1974) Autoxidation of native oxymyoglobin from bovine heart muscle, *Arch. Biochem. Biophys. 163*, 476−481.
8. Tsutsui, M., and Srivastava, T. S. (1973) Induced redox reactions of metalloporphyrins and their implications in biological systems, *Ann. N.Y. Acad. Sci. 206*, 404−408.
9. Wallace, W. J., Houtehens, R. B., Maxwell, J. C., and Caughey, W. S. (1982) Mechanism of autoxidation for hemoglobins and myoglobins, *J. Biol. Chem. 257*, 4966−4977.
10. Kanner, J., German, J. B., and Kinsella, J. E. (1987) Initiation of lipid peroxidation in biological systems, *Crit. Rev. Food Nutr. 25*, 317−364.
11. Brantley, R. E., Smerdson, S. J., Wilkinson, A. J., Singleton, E. W., and Otson, S. O. (1993) The mechanism of autoxidation of myoglobin, *J. Biol. Chem. 268*, 6995−7010.
12. Browne, P., Shalev, O., and Hebbel, R. P. (1998) The molecular pathobiology of cell membrane iron: the sickle red cell as a model, *Free Radical Biol. Med. 24*, 1040−1048.
13. Gorelik, S., and Kanner, J. (2001) Oxymyoglobin oxidation and membranal lipid peroxidation initiated by iron redox cycle, *J. Agric. Food Chem. 49*, 5945−5950.
14. Arduini, A., Eddy, L., and Hochstein, P. (1990) Detection of ferryl myoglobin in the isolated ischemic rat heart, *Free Radical Biol. Med. 9*, 511−513.
15. Svistunenko, D. A., Patel, R. P., and Wilson, M. T. (1996) An EPR investigation of human methaemoglobin oxidation by hydrogen peroxide: methods to quantify all paramagnetic species observed in the reaction, *Free Radical Res. 24*, 269−280.
16. Rice, R. H., Lee, Y. M., and Brown, W. D. (1983) Interactions of heme proteins with hydrogen peroxide: protein cross-linking and covalent binding of benzo[*a*]pyrene and 17 β-estradiol, *Arch. Biochem. Biohpys. 221*, 417−427.
17. Grisham, M. B. (1985) Myoglobin-catalyzed hydrogen peroxide dependent arachidonic acid peroxidation, *J. Free Radical Biol. Med. 1*, 227−232.
18. Kanner, J., and Harel, S. (1985) Initiation of membranal lipid peroxidation by activated metmyoglobin and methemoglobin, *Arch. Biochem. Biophys. 237*, 314−321.
19. Gutteridge, J. M. C. (1986) Iron promoter of the fenton reaction and lipid peroxidation can be released from hemoglobin by peroxides, *FEBS Lett. 201*, 291−295.
20. Harel, S., Salan, M. A., and Kanner, J. (1988) Iron release from metmyoglobin, methemoglobin, and cytochrome C by a system generating hydrogen peroxide, *Free Radical Res. Comm. 5*, 11−19.
21. Sakai, T., Kuwazuru, S., Yamauchi, K., and Uchida, K. (1995) A lipid oxidation-derived aldehydes, 4-hydroxy-2-nonenal, and omega 6 fatty acids contents in meats, *Biosci. Biotech. Biochem. 59*, 1379−1380.
22. Esterbauer, H., Schaur, R. J., and Zollner, H. (1991) Chemistry and biochemistry of 4-hydroxynonenal, malonaldehyde, and related aldehydes, *Free Radical Biol. Med. 11*, 81−128.
23. Frankel, E. N. (1987) Lipid oxidation: Mechanisms, products and biological significance, *J. Am. Oil Chem. Soc. 61*, 1908−1916.
24. Pryor, W. A., and Porter, N. A. (1990) Suggested mechanisms for the production of 4-hydroxy-2-nonenal from the autoxidation of polyunsaturated fatty acids, *Free Radical Biol. Med. 8*, 541−544.
25. Schneider, C., Tallman, K. A., Porter, N. A., and Brash, A. R. (2001) Two distinct pathways of formation of 4-hydroxynonenal, *J. Biol. Chem. 276*, 20831−20838.
26. Esterbauer, H. (1982) Aldehydic products of lipid oxidation, in *Free Radicals, Lipid Peroxidation and Cancer*, New York Academic Press, New York.
27. Blasig, I. E., Grune, T., Schonheit, K., Rohde, E., Jakstadt, M., Haseloff, R. F., and Siems, W. G. (1995) 4-Hydroxynonenal, a novel indicator of lipid peroxidation for reperfusion injury of the myocardium, *Am. J. Physiol. 269*, H14−H22.
28. Szweda, L. I., Uchida, K., Tsai, L., and Stadtman, E. R. (1993) Inactivation of glucose-6-phosphate dehydrogenase by 4-hydroxy-2-nonenal, *J. Biol. Chem. 268*, 3342−3347.
29. Millar, A. H., and Leaver, C. J. (2000) The cytotoxic lipid peroxidation product, 4-hydroxy-2-nonenal, specifically inhibits decarboxylating dehydrogenases in the matrix of plant mitochondria, *FEBS Lett. 481*, 117−121.
30. Gardner, H. W., and Deighton, N. (2001) Effect of 4-hydroxy-2(*E*)-nonenal on soybean lipoxygenase-1, *Lipids 36*, 623−628.
31. Patel, M. S., and Korotchkina, L. G. (2002) Pyruvate dehydrogenase complex as a marker of mitochondrial metabolism. Inhibition by 4-hydroxy-2-nonenal, *Methods Mol. Biol. 186*, 255−263.
32. Crabb, J. W., O'Neil, J., Miyagi, M., West, K., and Hoff, H. F. (2002) Hydroxynonenal inactivates cathepsin B by forming Michael adducts with active site residues, *Protein Sci. 11*, 831−840.
33. Uchida, K., and Stadtman, E. R. (1992) Modification of histidine residues in proteins by reaction with 4-hydroxynonenal, *Proc. Natl. Acad. Sci. U.S.A. 89*, 4544−4548.
34. Bolgar, M. S., Yang, C. Y., and Gaskell, S. J. (1996) First direct evidence for lipid/protein conjugation in oxidized human low-density lipoprotein, *J. Biol. Chem. 271*, 27999−28001.
35. Yla-Herttuala, S., Palinski, W., Rosenfeld, M. E., Parthasarathy, S., Carew, T. E., Butler, S., Witztum, J. L., and Steinberg, D. (1989) Evidence for the presence of oxidatively modified low-

density lipoprotein in atherosclerotic lesions of rabbit and man, *J. Clin. Invest. 84*, 1086−1095.
36. Takeda, A., Smith, M. A., Avila, J., Nunomura, A., Siedlak, S., Zhu, X., Perry, G., and Sayre, L. M. (2000) In Alzheimer's disease, heme oxygenase is coincident with Alz50, an epitope of τ induced by 4-hydroxy-2-nonenal modification, *J. Neurochem. 75*, 1234−1241.
37. McGrath, L. T., McGleenon, B. M., Brennan, S., McColl, D., McIlroy, S., and Passmore, A. P. (2001) Increased oxidative stress in Alzheimer's disease as assessed with 4-hydroxynonenal but not malondialdehyde, *Q. J. Med. 94*, 485−490.
38. Gotz, M. E., Wacker, M., Luckhaus, C., Wanek, P., Tatschner, T., Jellinger, K., Leblhuber, F., Ransmayr, G., Riederer, P., and Eder, E. (2002) Unaltered brain levels of 1,N^2-propanodeoxyguanosine adducts of *trans*-4-hydroxy-2-nonenal in Alzheimer's disease, *Neurosci. Lett. 324*, 49−52.
39. Yoritaka, A., Hattori, N., Uchida, K., Tanaka, M., Stadtman, E. R., and Mizuno, Y. (1996) Immunohistochemical detection of 4-hydroxynonenal protein adducts in Parkinson's disease, *Proc. Natl. Acad. Sci. 93*, 2696−2701.
40. Mak, S., Lehotay, D. C., Yazdanpanah, M., Azevedo, E. R., Liu, P. P., and Newton, G. E. (2000) Unsaturated aldehydes including 4-OH-nonenal are elevated in patients with congestive heart failure, *J. Card. Failure 6*, 108−114.
41. Toyukuni, S., Yamada, S., Kashima, M., Ihara, Y., Yamada, Y., Tanaka, T., Hiai, H., Seino, Y., and Uchida, K. (2000) Serum 4-hydroxy-2-nonenal-modified albumin is elevated in patients with type 2 diabetes mellitus, *Antioxid. Redox. Signal 2*, 681−685.
42. Tanaka, N., Tajima, S., Ishibashi, A., Uchida, K., and Shigematsu, T. (2001) Immunohistochemical detection of lipid peroxidation products, protein-bound acrolein, and 4-hydroxynonenal protein adducts, in actinic elastosis of photodamaged skin, *Arch. Dermatol. Res. 293*, 363−367.
43. Yu, B. P. (1994) Cellular defenses against damage from reactive oxygen species, *Physiol. Rev. 74*, 139−162.
44. Khan, M. F., Wu, X., Tipnis, U. R., Ansari, G. A. S., and Boor, P. J. (2002) Protein adducts of malondialdehyde and 4-hydroxynonenal in livers of iron loaded rats: quantitation and localization, *Toxicology 173*, 193−201.
45. Anton, R. M., Salgus, C., and Renerre, M. (1993) The study of oxidative reactions with lipid membranes and myoglobin in vitro, *Sci. Aliments 13*, 261−274.
46. Yin, M. C., and Faustman, C. (1994) The influence of microsomal and cytosolic components on the oxidation of myoglobin and lipid in vitro, *Food Chem. 51*, 159−164.
47. Faustman, C., Liebler, D. C., McClure, T. D., Sun, Q. (1999) α,β-Unsaturated aldehydes accelerate oxymyoglobin oxidation, *J. Agric. Food Chem. 47*, 3140−3144.
48. Yin, M. C., Faustman, C., Riesen, J. W., and Williams, S. N. (1993) Tocopherol and ascorbate delay oxymyoglobin and phospholipids oxidation in vitro, *J. Food Sci. 58*, 1273−1276.
49. Chan, W. K. M., Hakkarainen, K., Faustman, C., Schaefer, D. M., Scheller, K. K., and Liu, Q. (1996) Effect of dietary vitamin E supplementation on microbial load and sensory assessment in different beef cuts, *Meat Sci. 42*, 387−399.
50. Chan, W. K. M., Faustman, C., and Decker, E. A. (1997) Oxymyoglobin oxidation as affected by oxidation products of phosphatidylcholine liposomes, *J. Food Sci. 62*, 709−712.
51. Faustman, C., Cassens, R. G., Schaefer, D. M., Buege, D. R., Williams, S. N., and Scheller, K. K. (1989) Improvement of pigment and lipid stability in Holstein steer beef by dietary supplementation of vitamin E, *J. Food Sci. 54*, 858−862.
52. Arnold, R. N., Arp, S. C., Scheller, K. K., Williams, S. N., and Schaefer, D. M. (1993) Tissue equilibration and subcellular distribution of vitamin E relative to myoglobin and lipid oxidation in displayed beef, *J. Anim. Sci. 71*, 105−118.
53. Buttriss, J. L., and Diplock, A. T. (1988) The relationship between α-tocopherol and phospholipid fatty acids in rat liver subcellular membrane fractions, *Biochim. Biophys. Acta 962*, 81−90.
54. Liebler, D. C., and Burr, J. A. (1995) Antioxidant stoichiometry and the oxidative fate of vitamin E in peroxyl radical scavenging reactions, *Lipids. 30*, 789−793.
55. Wang, X., and Quinn, P. J. (1999) Vitamin E and its function in membranes, *Prog. Lipid Res. 38*, 309−336.
56. Bolgar, M. S., and Gaskell, S. J. (1996) Determination of the sites of 4-hydroxy-2-nonenal adduction to protein by electrospray tandem mass spectrometry, *Anal. Chem, 68*, 2325−2330.
57. Lynch, M. P., and Faustman, C. (2000) Effect of aldehydes lipid oxidation products on myoglobin, *J. Agric. Food Chem. 48*, 600−604.
58. Faustman, C., and Phillips, A. L. (2001) Measurement of discoloration in fresh meat, Ch. F3 Unit F3.3 in *Current Protocols in Food Analytical Chemistry*, Wiley and Sons, Inc., New York.
59. Krzywicki, K. (1982) The determination of haem pigments in meat, *Meat Sci. 7*, 29−36.
60. Fritz, J. D., Swartz, D. R., and Greaser, M. L. (1989) Factors affecting polyacrylamide gel electrophoresis of high-molecular-weight myofibrillar proteins, *Anal. Biochem. 180*, 205−210.
61. Fritz, J. D., and Greaser, M. L. (1991) Changes in titin and nebulin in post mortem bovine muscle revealed by gel electrophoresis, Western blotting, and immunofluorescence microscopy, *J. Food Sci. 56*, 607−610.
62. Waeg, G., Dimsity, G., and Esterbauer, H. (1996) Monoclonal antibodies for detection of 4-hydroxynone, *Free Radical Res. 25*, 149−159.
63. Yates, J. R. (1998) Mass spectrometry and the age of the proteome, *J. Mass Spec. 33*, 1−19.
64. Hansen, B. T., Jones, J. A., Mason, D. E., and Liebler, D. C. (2001) SALSA: A pattern recognition algorithm to detect electrophile-adducted peptides by automated evaluation of CID spectra in LC−MS−MS analyses, *Anal. Chem. 73*, 1676−1683.
65. Liebler, D. C., Hansen, B. T., Davey, S. W., Tiscareno, L., and Mason, D. E. (2002) Peptide sequence motif analysis of tandem MS data with the SALSA algorithm, *Anal. Chem. 74*, 203−210.
66. SAS (1985) *SAS user guide: statistics*, 5th ed., SAS Institute, Cary, NC.
67. Lee, S., Phillips, A. L., Liebler, D. C., and Faustman, C. (2003) Porcine oxymyoglobin and lipid oxidation in vitro, *Meat Sci. 63*, 241−247.
68. Barrick, D., Hughson, F. M., and Baldwin, R. L. (1994) Molecular mechanisms of acid denaturation. The role of histidine residues in the partial unfolding of apomyoglobin, *J. Mol. Biol. 237*, 588−601.
69. Livingston, D. J., and Brown, W. D. (1981) The chemistry of myoglobin and its reaction, *Food Technol. 35*, 244−252.
70. Badghisi, H., and Liebler, D. C. (2002) Sequence mapping of epoxide adducts in human hemoglobin with LC-Tandem MS and the salsa algorithm, *Chem. Res. Toxicol*. 15, 799−805.

BI0271695